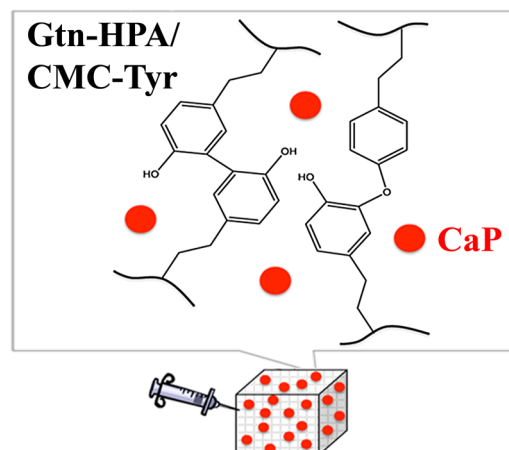


A Periosteum-Inspired 3D Hydrogel-Bioceramic Composite for Enhanced Bone Regeneration^a

Yong Yao Chun, Jun Kit Wang, Nguan Soon Tan, Peggy Puk Yik Chan, Timothy Thatt Yang Tan,* Cleo Choong*

A 3D injectable hydrogel-bioceramic composite consisting of gelatin-3-(4-hydroxyphenyl) propionic acid (Gtn-HPA) and carboxymethyl cellulose-tyramine (CMC-Tyr), incorporated with fish scale-derived calcium phosphate (CaP), is developed for bone applications. The hydrogel-bioceramic composite has significantly improved the elastic modulus compared to the non-filled hydrogel, of which the addition of 10 w/v% CaP showed zero order fluorescein isothiocyanate (FITC)-dextran release profile and a significantly higher proliferation rate of encapsulated cells. All the samples promote the nucleation and growth of CaP minerals when exposed to 1× SBF. Overall, the hydrogel-bioceramic composite with 10 w/v% CaP can potentially be used as a periosteum-mimicking membrane to facilitate bone regeneration.

Hydrogel-bioceramic composite



Prof. T. T. Y. Tan, Y. Y. Chun
School of Chemical and Biomedical Engineering, Nanyang Technological University, 62 Nanyang Drive, Singapore 637459, Singapore
E-mail: tytan@ntu.edu.sg
Prof. C. Choong
School of Materials Science and Engineering, Nanyang Technological University, 50 Nanyang Avenue, Singapore 639798, Singapore
Prof. C. Choong, Prof. N. S. Tan
KK Research Centre, KK Women's and Children Hospital, 100 Bukit Timah Road, Singapore 229899
J. K. Wang
Residues and Resource Reclamation Centre (R3C), Nanyang Environment and Water Research Institute (NEWRI), Nanyang Technological University, 1 Cleantech Loop, Singapore 637141, Singapore

J. K. Wang
Interdisciplinary Graduate School, Nanyang Technological University, 50 Nanyang Avenue, Singapore 639798, Singapore
Prof. N. S. Tan
School of Biological Science, Nanyang Technological University, 60 Nanyang Drive, Singapore 637551, Singapore
Prof. N. S. Tan
Institute of Molecular and Cell Biology, 61 Biopolis Drive, Proteos, A*STAR, Singapore 138673, Singapore
Dr. P. P. Y. Chan
Department of Telecommunications Electrical Robotics and Biomedical Engineering, Swinburne University of Technology, Hawthorn, Victoria 3122, Australia
Dr. P. P. Y. Chan
Melbourne Centre for Nanofabrication, Clayton 3168, Australia

^aSupporting Information is available online from the Wiley Online Library or from the author.

1. Introduction

Bone grafts are crucial in orthopaedic reconstruction due to the large number of cases of traumatic injuries, tumor resections, and birth defects that cause large bone defects.^[1] Among the different types of bone grafts, autografts remain the gold standard due to good osteointegrative, osteoconductive, osteoinductive, and osteogenic properties.^[2] However, the drawback of autografts is the limited amount of graft material that can be extracted from the patient's own body. Also, harvesting the graft material from the patient itself can cause donor site morbidity.^[3] Thus, synthetic bone grafts have become a more attractive grafting material for large bone defects. Although synthetic bone grafts can provide large graft volume, most of these grafts do not contain osteogenic properties that are essential for bone healing.^[4] In comparison, autografts have better bone regeneration properties as they consist of living cells, growth factors, and osteogenic substances that are found in the periosteum on the autograft surface. This periosteum contributes osteoinductive and osteogenic properties to the autograft and is able to induce osteogenic differentiation of stem cells that lead to formation of new bone.^[5] For this reason, there is a need to create a system that mimics the periosteum to provide osteoinductive and osteogenic properties for the synthetic bone graft, so as to enhance bone healing efficiency for large bone defect reconstruction.

Several studies have reported the fabrication of periosteum-mimicking membrane using stem cell-engineered cell sheets and stem cell encapsulated hydrogel. However, the cell sheet technology used to enhance bone healing is not fully understood, while the hydrogel has a slow healing rate compared to an autograft mainly due to the lack of an osteogenic component.^[6,7] As such, incorporation of bioactive calcium phosphate (CaP) powder into the hydrogel system could promote the osteogenic differentiation of the stem cells to facilitate defect closure and new bone tissue formation as well as improving the mechanical properties of the hydrogel system.^[8,9] Thus, a cell encapsulating injectable hydrogel-bioceramic composite with bioactive components and tunable porosity could be more suitable as a bone patch to mimic the periosteum. The use of post-implantation pore tunability of the hydrogel-bioceramic composite could facilitate cell penetration and tissue ingrowth to accommodate differential healing rate.^[10]

The current work, inspired by the regenerative functionality of the periosteum, aims to develop and investigate a new hydrogel-bioceramic composite, based on a previous gelatin-3-(4-hydroxyphenyl) propionic acid (Gtn-HPA) and carboxymethyl cellulose-tyramine (CMC-Tyr) hydrogel system developed by our group, and incorporated with fish scale-derived CaP to develop the periosteum-mimicking membrane to provide osteoinductive and osteogenic

properties for bone regeneration. The Gtn-HPA/CMC-Tyr hydrogel is biocompatible and possesses post-implantation pore tailorability property that enables on-demand host tissue ingrowth and blood vessels infiltration.^[10] Fish scale-derived CaP was chosen for this study as it is an abundant biowaste with a simple extraction process in addition to its excellent biocompatibility, bioactivity, and high osteoconductivity. Most importantly, this naturally derived CaP compound is non-toxic and has non-inflammatory/non-immunogenic properties when compared with the chemically synthesized CaP.^[11,12] The fish scale-derived CaP has also been shown to be similar to the bone mineral, which is a substituted hydroxyapatite, in term of chemical properties, making it a suitable source for providing osteogenic properties for bone integration and repair.^[13] In this work, the effect of CaP on the properties of the Gtn-HPA/CMC-Tyr hydrogel was investigated in terms of mechanical properties, drug delivery efficacy, in situ mineral formation, and cell proliferation, in order to examine the potential of the proposed hydrogel-bioceramic composite in enhancing bone graft healing efficiency as a periosteum-mimicking membrane.

2. Experimental Section

2.1. Isolation and Characterization of Fish Scale-Derived Calcium Phosphate

Fish scales from snakeheads (*Channa argus*) were obtained from Khai Seng Trading and Fish Farm Pte Ltd., Singapore. Fish scales were cleaned with deionized (DI) water and heated at a constant rate of $10\text{ }^{\circ}\text{C}\cdot\text{min}^{-1}$ to $850\text{ }^{\circ}\text{C}$ and kept at this constant temperature for an hour. The heat-treated fish scales were milled evenly to obtain CaP powder. The CaP powder was characterized using Fourier transform infrared spectroscopy (Frontier FTIR; PerkinElmer Instrument, USA) to identify the chemical bonds and X-ray diffractometry (XRD; Shimadzu XRD-6000, Shimadzu Corp., Japan) to identify the CaP phases. The FTIR spectrum was scanned for region from 4000 to 650 cm^{-1} with a scan number of 32, while the XRD was characterized using $\text{CuK}\alpha$ -radiation ($\lambda = 1.5406\text{ \AA}$) via theta/2theta mode ($20 < 2\theta < 60$) with a step size of 0.05° at scan speed of $1^{\circ}\cdot\text{min}^{-1}$. The morphology and the calcium-to-phosphate ratio (Ca/P ratio) of the CaP powder was characterized using scanning electron microscope (SEM; JSM-6360LV, JEOL Corp., Japan) equipped with energy-dispersive X-ray spectroscopy (EDX). The CaP powder was coated with a thin layer of gold using sputter coater (Structure Probe, Inc., USA) for 90 s and then imaged using a voltage of 20 kV.

2.2. Synthesis of Hydrogel Precursors

Gtn-HPA and CMC-Tyr conjugates were synthesized according to previously established procedures.^[14] Briefly, for the synthesis of Gtn-HPA conjugate, 3.32 g of 3-(4-hydroxyphenyl) propionic acid (HPA; 98%, Sigma-Aldrich, USA) and 3.20 g *N*-hydroxysuccinimide

(NHS; 98%, Sigma–Aldrich, USA) were first dissolved in 150 ml DI water mixed with 100 ml of *N,N*-dimethylformamide (DMF; anhydrous 99.8%, Sigma–Aldrich, USA). 3.82 g of *N*-(3-dimethylaminopropyl)-*N'*-ethylcarbodiimide hydrochloride crystalline (EDC; Sigma–Aldrich, USA) were added to this solution. The pH of the mixture was adjusted to 4.7. Then, a 6.67 weight per volume percent (w/v%) gelatin (Wako Pure Chemical Industries, Japan) solution was added to this mixture where the reaction was allowed to take place overnight at room temperature. After the reaction processed, the mixture was dialyzed against 0.1 M sodium chloride (NaCl; BioXtra, ≥99.5%, Sigma–Aldrich, USA) followed by 25% ethanol (absolute grade, Merck, Germany) and lastly using DI water in sequence for 2 d each. The mixture was lyophilized to get the final product. For synthesizing of CMC-Tyr conjugate, 5 g of sodium carboxymethyl cellulose (CMC; average $M_w \approx 90\,000$, Sigma–Aldrich, USA) was dissolved in 250 ml of DI water. 0.8648 g of tyramine chloride (≥98%, Sigma–Aldrich, USA), 0.5732 g of NHS, and 0.9547 g of EDC were then added to this solution to initiate the reaction. The pH value of the mixture was adjusted to 4.7, and the reaction was allowed to take place overnight. After the conjugation reaction was completed, the mixture was dialyzed against 0.1 M NaCl, 25% ethanol, and finally with DI water in that order for 2 d each prior to lyophilization. ^1H -nuclear magnetic resonance spectroscopy (NMR; Bruker Avance 300 MHz, Bruker Instruments, Inc., USA) was used to characterize the success of conjugation of phenol molecules on Gtn and CMC. Proton nuclear magnetic resonance (^1H NMR) spectra were recorded from the liquid sample with a concentration of $10\text{ mg} \cdot \text{ml}^{-1}$ in deuterium oxide (D_2O ; 99.9 atom% D, Sigma–Aldrich, USA).

2.3. Fabrication of the Hydrogel-Bioceramic Composite (Gtn-HPA/CMC-Tyr/CaP)

The lyophilized Gtn-HPA and CMC-Tyr conjugates were dissolved separately in $1 \times$ PBS to form a 5 w/v% polymer solution. The hydrogel precursor was formed by mixing the Gtn-HPA and the CMC-Tyr solutions at a volume ratio of 4:1. The hydrogel precursor was cross-linked using $0.15\text{ U} \cdot \text{ml}^{-1}$ horseradish peroxidase (HRP; $100\text{ U} \cdot \text{mg}^{-1}$, Wako Pure Chemical Industries, Japan) and 1.5 mM hydrogen peroxide (H_2O_2 ; 30 wt%, Wako Pure Chemical Industries, Japan). The 3D hydrogel-bioceramic composite (Gtn-HPA/CMC-Tyr/CaP) was fabricated by mixing different amount (w/v%) of fish scale-derived CaP into the hydrogel precursor solution. The mixture was vortexed to ensure an even dispersion of CaP prior to cross-link with HRP and H_2O_2 .

2.4. Morphology and Pore Size Studies

The cross-sectional structures of lyophilized samples were characterized by scanning electron microscopy (SEM; JSM-6360LV, JEOL Corp., Japan) using the same conditions as previously described in Section 2.1 using a voltage of 10 kV.

2.5. Mechanical Properties Characterization

For the mechanical properties study, both the non-filled Gtn-HPA/CMC-Tyr hydrogel and the hydrogel-bioceramic composites were

cast into a 13 mm diameter mold using 1.5 ml of precursor solution with a cross-linker amount of $0.15\text{ U} \cdot \text{ml}^{-1}$ HRP and 1.5 mM H_2O_2 , forming a cylindrical scaffold with a final height of 11.5 mm. The mechanical properties of the samples ($n = 4$) were measured by using a mechanical testing machine (Instron 5567, Instron, USA) with a load cell of 10 N at a constant rate of $0.02\text{ mm} \cdot \text{s}^{-1}$ compressed to 50% of the sample's height. The elastic modulus of samples was obtained from the linear portion of stress–strain curve.

2.6. Swelling Ratio

To investigate the swelling ratio of the sample, both the non-filled Gtn-HPA/CMC-Tyr hydrogel and the hydrogel-bioceramic composites were immersed into $1 \times$ PBS and incubated at 37°C for 7 d. The swelling ratio of the non-filled Gtn-HPA/CMC-Tyr hydrogel and the hydrogel-bioceramic composites was calculated using Equation (1):

$$\text{Swelling ratio} = \frac{W_w - W_d}{W_d} \times 100\% \quad (1)$$

where W_d is the dry weight of lyophilized sample and W_w is the wet weight of the sample after soaking in $1 \times$ PBS for day 1, 4, and 7 at 37°C .

2.7. Drug Release Study

Fluorescein isothiocyanate (FITC)-dextran (average mol wt. 20 000, Sigma–Aldrich, USA) was first mixed with 1 ml of the sample precursor (non-filled Gtn-HPA/CMC-Tyr hydrogel or hydrogel-bioceramic composites) with a concentration of $20\text{ }\mu\text{g} \cdot \text{ml}^{-1}$ and then cross-linked using $0.15\text{ U} \cdot \text{ml}^{-1}$ HRP and 1.5 mM H_2O_2 . The samples containing FITC-dextran were allowed to set in 24-well plate for 2 h to form a cylindrical shape hydrogels. The samples were then immersed in 1 ml of $1 \times$ PBS solution and incubated at 37°C . Every 1 h, $200\text{ }\mu\text{l}$ of $1 \times$ PBS solution from each well plate was taken out and scanned using microplate reader (SpectraMax M2, Molecular Devices, USA) under the fluorescence mode with an excitation wavelength of 495 nm, emission wavelength of 519 nm, and emission cut-off at 515 nm. Each sample was scanned with 20 flashes per read. The fluorescence intensity of the sample at each time point was compared using a standard curve correlating the known FITC-dextran concentrations with fluorescence. The FITC-dextran initial release test was carried out for 6 h. Subsequently, the readings were continuously taken every 24 h until a plateau was reached for the full release study.

2.8. Enzymatic Degradation Study

Both the non-filled Gtn-HPA/CMC-Tyr hydrogel and the hydrogel-bioceramic composites were cast into the Petri dish (diameter = 35 mm, height 10 mm) using 2 ml of precursor solution cross-linked with $0.15\text{ U} \cdot \text{ml}^{-1}$ HRP and 1.5 mM H_2O_2 . The enzymatic reaction was allowed to proceed for 2 h to ensure complete cross-linking. The samples were immersed in 2 ml of $1 \times$ PBS solution that contained $0.70\text{ U} \cdot \text{ml}^{-1}$ of type-I collagenase (Life Technologies, USA) and then incubated at 37°C and shook at 60 rpm using the orbital shaker

(Bibby Sterilin Ltd., England). The percentage weight change of the non-filled Gtn-HPA/CMC-Tyr hydrogel and the hydrogel-bioceramic composites was calculated using Equation (2):

$$\text{Percentage weight change} = \frac{W_o - W_t}{W_o} \times 100\% \quad (2)$$

where W_o is the initial weight of the sample and W_t is the sample weight at specific time point. At each time point, the samples were removed from the solution, blotted dry to remove excess solution at the surface, and weighed. The degradation study was carried out hourly for 8 h.

2.9. Biomineralization Study

Non-filled Gtn-HPA/CMC-Tyr hydrogel and hydrogel-bioceramic composites were cross-linked using 0.15 U · ml⁻¹ HRP and 1.5 mM H₂O₂ and cast in a 48-well plate using 0.5 ml of the solution. The samples were pre-treated using 200 mM calcium chloride (CaCl₂ · 2H₂O; Sigma-Aldrich, USA) and 200 mM potassium hydrogen phosphate trihydrate (K₂HPO₄ · 3H₂O; Sigma-Aldrich, USA) prior to simulated body fluid (SBF) treatment. 1× SBF was prepared according to Kokubo et al. (1990). In brief, 7.996 g NaCl, 0.350 g sodium bicarbonate (NaHCO₃; Sigma-Aldrich, USA), 0.224 g potassium chloride (KCl; Sigma-Aldrich, USA), 0.228 g potassium phosphate dibasic trihydrate (K₂HPO₄ · 3H₂O; Sigma-Aldrich, USA), and 0.305 g magnesium chloride hexahydrate (MgCl₂ · 6H₂O; Sigma-Aldrich, USA) were dissolved in 1 L of DI water. Then, 40 ml of 1 M hydrochloric acid (HCl; 37%, Merck, Germany) was added into solution before dissolving 0.278 g calcium chloride (CaCl₂; Sigma-Aldrich, USA), 0.071 g sodium sulfate (Na₂SO₄; Sigma-Aldrich, USA) and 6.057 g tris(hydroxymethyl) aminomethane ((CH₂OH)₃CNH₂; Sigma-Aldrich, USA) into the solution.^[15] The pH of the solution was adjusted using 10 M HCl to 7.25 to get a clear solution. The samples were then soaked in 1× SBF, incubated at 37 °C. The 1× SBF solution was changed on a daily basis. On days 1 and 7, respectively, the samples were removed from the solution, washed with DI water three times, and lyophilized. The lyophilized samples were then characterized using SEM-EDX (JSM-6360LV, JEOL Corp., Japan) under the same conditions as previously described in Section 2.1 and voltage of 10 kV to study its morphology and the Ca/P ratio. The Ca/P ratio was obtained from an average of three regions from three different samples ($n = 9$).

2.10. 3D Cell Encapsulation Study

The polymer solutions containing 5 w/v% Gtn-HPA or 5 w/v% CMC-Tyr conjugates were prepared in Dulbecco's Modified Eagle Medium (DMEM; Life Technologies, USA) together with 10% fetal bovine serum (FBS; Thermo Scientific, USA) and 1× antibiotic-antimycotic (ABAM; Life Technologies, USA). The hydrogel precursor was then filter sterilized using a 0.22 μm filter syringe. Hydrogel precursor was prepared by mixing the Gtn-HPA and the CMC-Tyr solutions at a volume ratio of 4:1. Fish scale-derived CaP powder was stabilized by treating with DMEM in order for the powder to reach physiological pH. Different w/v% CaP was then mixed with the Gtn-HPA/CMC-Tyr hydrogel precursor solution to form a Gtn-HPA/CMC-Tyr/CaP precursor solution. Human embryonal kidney 293FT

cells, were then mixed with the precursor solution at a cell density of 5 × 10⁴ cells · ml⁻¹. 0.5 ml non-filled Gtn-HPA/CMC-Tyr hydrogel and hydrogel-bioceramic composites were then formed in 24-well plate by adding 0.15 U · ml⁻¹ HRP and 1.5 mM H₂O₂. The cell proliferation rate was measured using PrestoBlue cell viability reagent (Life Technologies, USA) on days 1, 3, 5, and 7. LIVE/DEAD cell viability assay (Life Technologies, USA) was used to observe live and dead cells encapsulated inside the hydrogel on day 7 using the Zeiss Axio Observer Z1 inverted microscope (Carl Zeiss, Germany).

2.11. Statistical Analysis

All data are expressed in mean ± standard deviation with a replicate of $n = 3$, unless otherwise specific. The differences between the values were assessed using Kruskal–Wallis one-way analysis of variance and Mann–Whitney *U*-test, where $P < 0.05$ was considered statistically significant.

3. Results and Discussion

3.1. Characterization of Fish Scale-Derived Calcium Phosphate

In order to obtain the pure inorganic component from the fish scales, the scales were sintered at 850 °C. This temperature was used to avoid phase change of the fish scale's hydroxyapatite to β-tricalcium phosphate (β-TCP), which takes place beyond 850 °C.^[12] The sintered powder was characterized based on the chemical properties using FTIR, XRD, and SEM-EDX. From the FTIR analysis (Figure 1a), the presence of the strong characteristic peak for phosphate group (PO₄³⁻) located at ≈ 1 000 cm⁻¹ is an indication of the presence of CaP compound in the fish scale-derived powder sample. Further confirmation of the presence of CaP was carried out using XRD analysis (Figure 1b), in which the spectrum obtained for fish scale-derived powder sample closely resembles that of the spectrum of hydroxyapatite (spectrum was compared to “International Centre of Diffraction Data” according to Powder Diffraction File (PDF)). The result showed that the sintered powder consisted of monophase CaP compound and confirmed that the temperature used for sintering process only produced hydroxyapatite phase, but not both hydroxyapatite and β-TCP phases. From the SEM-EDX result (Figure 1c and d), fish scale-derived CaP has a Ca/P ratio of 1.75 ± 0.04, which is similar to the ratio for human bone mineral (Ca/P ratio of 1.55–1.75).^[16] Taken together, the fish scale-derived CaP possesses chemical properties such as resorption rate that closely matches that of the human bone, and is a suitable source for providing osteogenic properties for bone integration and repair in our hydrogel system.^[17] In addition, the sintering of fish scale is one of the simplest methods and fish scale is a low-cost source for natural CaP.

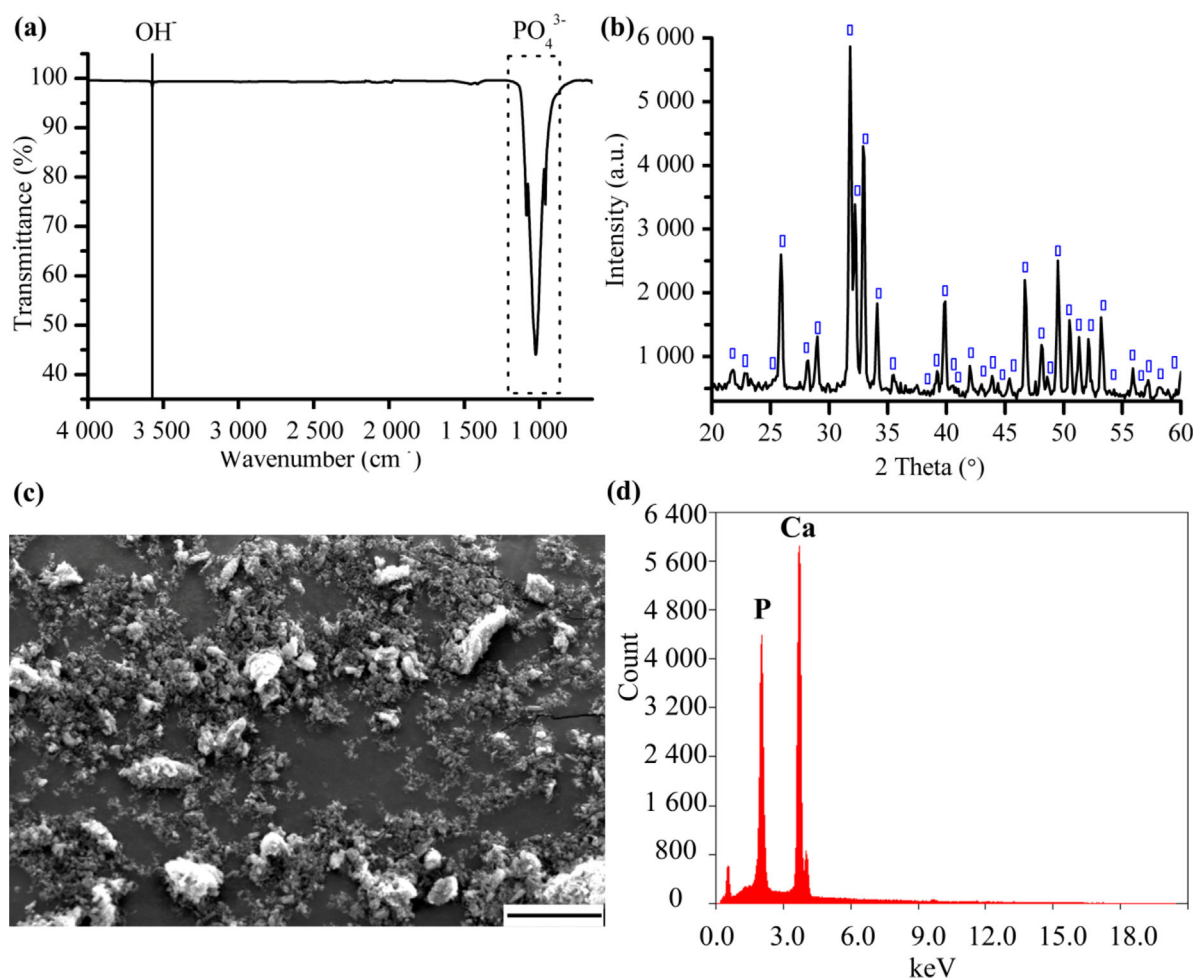


Figure 1. Surface characterization of fish scale-derived calcium phosphate by (a) ATR-FTIR analysis showing the characteristic peaks for calcium phosphate compounds (Solid line: hydroxyl group; Dotted box: phosphate group); (b) XRD analysis showing the diffraction peaks corresponding to hydroxyapatite (As indicated by the blue box) and (c,d) The representative morphology and chemical composition of fish scale-derived calcium phosphate by SEM-EDX showing the presence of calcium and phosphate elements. (Scale bar = 20 μm).

3.2. Fabrication of the Hybrid Hydrogel-Bioceramic System

In the hydrogel precursor synthesis process, the Gtn and CMC backbones were conjugated with small phenol molecules, HPA and Tyr, respectively, through a well-known carbodiimide/active ester mediated coupling reaction.^[10,18] When ^1H NMR spectroscopy was used to examine phenol conjugation onto the Gtn and CMC backbones, two additional peaks in the chemical shift region between δ 6.0 to 8.0 ppm were observed for both Gtn-HPA and CMC-Tyr respectively (Figure 2b and d), which is absent in the Gtn and CMC (Figure 2a and c). These two additional peaks corresponded to the two aromatic protons in the small phenol molecules, indicating successful conjugation of the small phenol molecules of HPA and Tyr onto the Gtn and CMC backbones respectively.^[19,20]

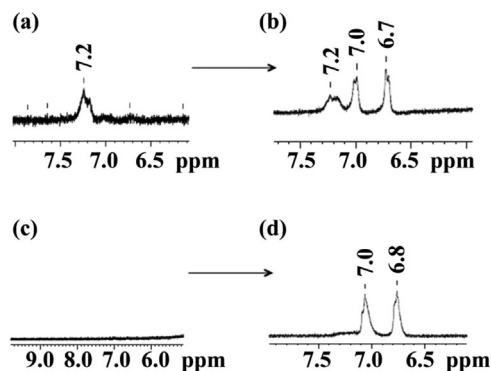


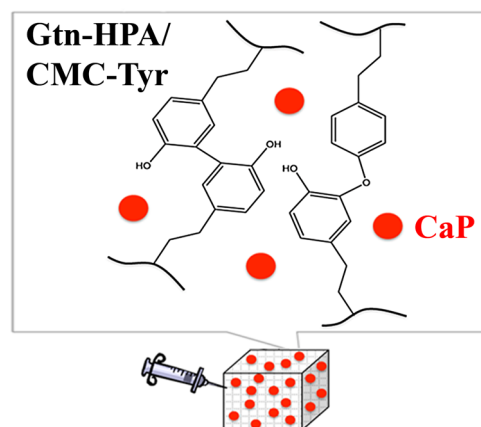
Figure 2. ^1H NMR spectrum for (a) Gtn, (b) Gtn-HPA, (c) CMC and (d) CMC-Tyr. The chemical shift in the region of δ 6.0–8.0 ppm indicates successful conjugation of the phenol group onto the gelatin and CMC, respectively.

The successful conjugation of phenol molecules onto the Gtn and CMC backbones enables cross-linking of Gtn and CMC through a peroxidase-mediated coupling reaction.^[21] This method of polymer cross-linking is favorable for bone tissue engineering application because the reaction can proceed under physiological conditions.^[10] In the current system, two types of polymers with different hydrophilicity are used to induce pore formation through phase separation. As cross-linking occurs over time, both polymers will phase separate to its discrete domain leading to pore formation in the hydrogel's structure.^[22] In general, pore formation is essential for cells to attach, grow, and migrate throughout the material.^[23]

3.3. Morphology of the Hybrid Hydrogel-Bioceramic System

When fish scale-derived CaP powder was mixed with the Gtn-HPA/CMC-Tyr hydrogel precursor, CaP powder was immobilized throughout the hydrogel matrix simultaneously as depicted in Scheme 1. The interior structure of the non-filled Gtn-HPA/CMC-Tyr hydrogel and the hydrogel-bioceramic composites were lyophilized and visualized using SEM (Figure 3) to allow for a better understanding of the CaP distribution and hydrogel morphology. In general, the lyophilized non-filled Gtn-HPA/CMC-Tyr hydrogel had a smooth surface and possessed large pores in the structure. Overall, the incorporation of CaP into the Gtn-HPA/CMC-Tyr hydrogel led to increase surface roughness, which promotes cell attachment, proliferation, and spreading, particularly for osteoblast cells, and thus can potentially enhance bone healing.^[24]

Hydrogel-bioceramic composite



Scheme 1. Schematic illustration of the fabrication process for the hydrogel-bioceramic composite, which involves the incorporation of fish scale-derived calcium phosphate powder into the precursor prior to enzyme cross-linking.

3.4. Mechanical Properties of the Hydrogel-Bioceramic Composite

The elastic modulus of the hydrogel-bioceramic composite prepared by cross-linking with $0.15 \text{ U} \cdot \text{ml}^{-1}$ HRP and 1.5 mM H_2O_2 , followed with mixing with different w/v% CaP, were measured, and the results shown in Figure 4a. In general, an increasing elastic modulus was observed with an increasing w/v% CaP incorporated into the hydrogels system. The elastic modulus for non-filled Gtn-HPA/CMC-Tyr hydrogel (0 w/v% CaP) was determined to be $1556.5 \pm 160.1 \text{ Pa}$. The elastic modulus increased significantly ($P < 0.05$) by 104.1%

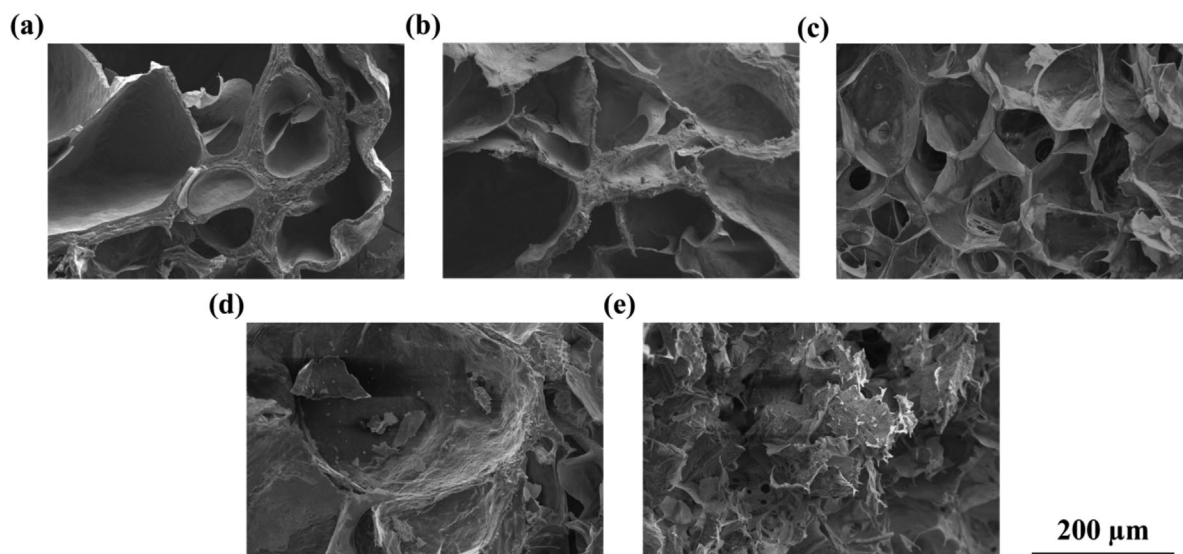


Figure 3. SEM images of lyophilized (a) non-filled Gtn-HPA/CMC-Tyr hydrogel and hydrogel-bioceramic composites with (b) 5, (c) 10, (d) 20, and (e) 40 w/v% CaP.

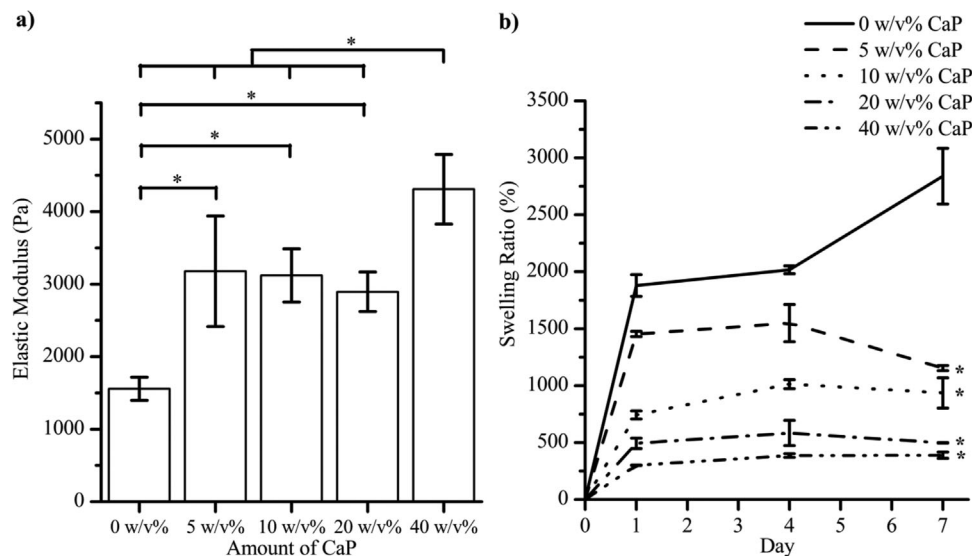


Figure 4. Graphs of (a) elastic modulus and (b) swelling ratio for hydrogels containing different amounts of calcium phosphate. (* $P < 0.05$).

and 100.5% when 5 and 10 w/v% CaP powder was incorporated into the Gtn-HPA/CMC-Tyr hydrogel system respectively, 86% for hydrogel-bioceramic composite with 20 w/v% CaP, and by 177% when 40 w/v% CaP powder was incorporated into Gtn-HPA/CMC-Tyr hydrogel. However, no significant difference across the CaP-enriched sample groups was observed except for the hydrogel-bioceramic composite with 40 w/v% CaP.

The elastic modulus of a scaffold is known to play a key role in directing stem cell differentiation into a specific cell lineage.^[25,26] For the hydrogel-bioceramic composite, there is an overall improvement of the mechanical strength of the hydrogel-bioceramic composite. A study by Sun et al., which examined the mechanical properties of scaffold on cell fate determination, showed that the increased of elastic modulus of gelatin scaffold from ≈ 0.6 kPa to ≈ 2.5 kPa through EDC cross-linking was able to promote early chondrogenic differentiation of stem cells followed by chondrogenic and osteogenic differentiation at the later stage.^[27] This is to mimic the endochondral ossification process, which is one of the two natural healing processes of bone that first involves the formation of bone callus. The incorporation of CaP into the non-filled Gtn-HPA/CMC-Tyr hydrogel improved the elastic moduli to the range ≈ 3 –5 kPa, and thus this system can be potentially applied as a periosteum-mimicking layer to assists in bone repair through providing the right mechanical environment to regulate cell fate.

The improved mechanical properties can be explained by the CaP powder acting as fillers to form a particle-reinforced composite. In addition, it is also suggested that the physical interaction between calcium ions (Ca^{2+}) of CaP with the free reactive sites of Gtn-HPA/CMC-Tyr polymers has contributed to the improvement on strength for the hydrogel-bioceramic

composite. A theoretical study by Reddy et al. demonstrated that Ca^{2+} forms strong cation- π interaction with aromatic groups.^[28] For our system, the aromatic groups from HPA, phenylalanine, and tyrosine residues in Gtn-HPA and the aromatic group from Tyr in CMC-Tyr contribute to interactions with the Ca^{2+} ions. This interfacial interaction possibly causes a physical cross-linking between different strands of Gtn and CMC and leads to improvement in the mechanical properties of the hydrogel-bioceramic composite.^[29] However, a different filler-matrix interaction was observed with varying amount of CaP. In this case, an exponential relationship was found between the CaP amount and the elastic modulus. Although the CaP served as a filler to improve the overall performance of the composite in particularly the elastic modulus of the composite, the filler interaction was weak when a small amount of CaP was added, which was not sufficient to transit from a gel-like material to a rigid material. As the amount of CaP increased, the filler-matrix interaction increased where a critical CaP concentration of 40 w/v% would significantly induce the transition of solid-like behavior of the hydrogel. This resulted in the exponential increase in the overall mechanical performance of the composite due to the reduction of dangling polymers and decreased in the cross-linking distance and thus the motion of the gel.^[30]

3.5. Swelling Capacity Measurements of the Hydrogel-Bioceramic Composite

As shown in Figure 4b, the non-filled Gtn-HPA/CMC-Tyr hydrogel has a swelling ratio of $2838.9 \pm 245.3\%$ at day 7, which decreased significantly ($P < 0.05$) to $1154.0 \pm 23.1\%$ when 5 w/v% CaP was incorporated within the Gtn-HPA/CMC-Tyr hydrogels. The swelling ratio continued to decrease

significantly ($P < 0.05$) as compared to non-filled Gtn-HPA/CMC-Tyr hydrogel to $936.0 \pm 132.8\%$, $497.2 \pm 110.1\%$, and $388.2 \pm 27.2\%$ when 10, 20, and 40 w/v% CaP was incorporated into the Gtn-HPA/CMC-Tyr hydrogels, respectively. The higher interaction between different polymer strands leads to a stiffer network and a decrease in the swelling ratio.^[30] The swelling ratio is indicative of the hydrogel's nutrient and waste exchange efficacy, since a large swelling ratio could facilitate more efficient transportation of nutrients and wastes. In general, there needs to be a balance between improved mechanical properties and swelling ratio in order to achieve an optimal system that has the appropriate mechanical environment and sufficient mass transport capabilities.

3.6. Drug Release Profile for the Hydrogel-Bioceramic Composite

FITC-dextran was used as the model drug to investigate the drug release profile of the hydrogel-bioceramic composite

with different amount of CaP. As shown in Figure 5, all the hydrogel-bioceramic composites had a zero-order release profile similar with the non-filled Gtn-HPA/CMC-Tyr hydrogel regardless of amount of CaP incorporated attributed to a diffusion-controlled release process. The FITC-dextran release kinetic of the hydrogel-bioceramic composite incorporated with 5 and 10 w/v% CaP showed a comparable release kinetics compared to non-filled Gtn-HPA/CMC-Tyr hydrogel. However, the hydrogel-bioceramic composite incorporated with 20 and 40 w/v% CaP exhibited an initial burst release of FITC-dextran with a significantly ($P < 0.05$) higher release rate compared to non-filled Gtn-HPA/CMC-Tyr hydrogel. The burst release for the hydrogel-bioceramic composite incorporated with 20 and 40 w/v% CaP might be associated with the different degradation behavior of the composite, which will be discussed in Section 3.7. Drug release from the hydrogels occurred at the same time when degradation took place as the hydrogels were exposed to the physiological solutions. It is suggested

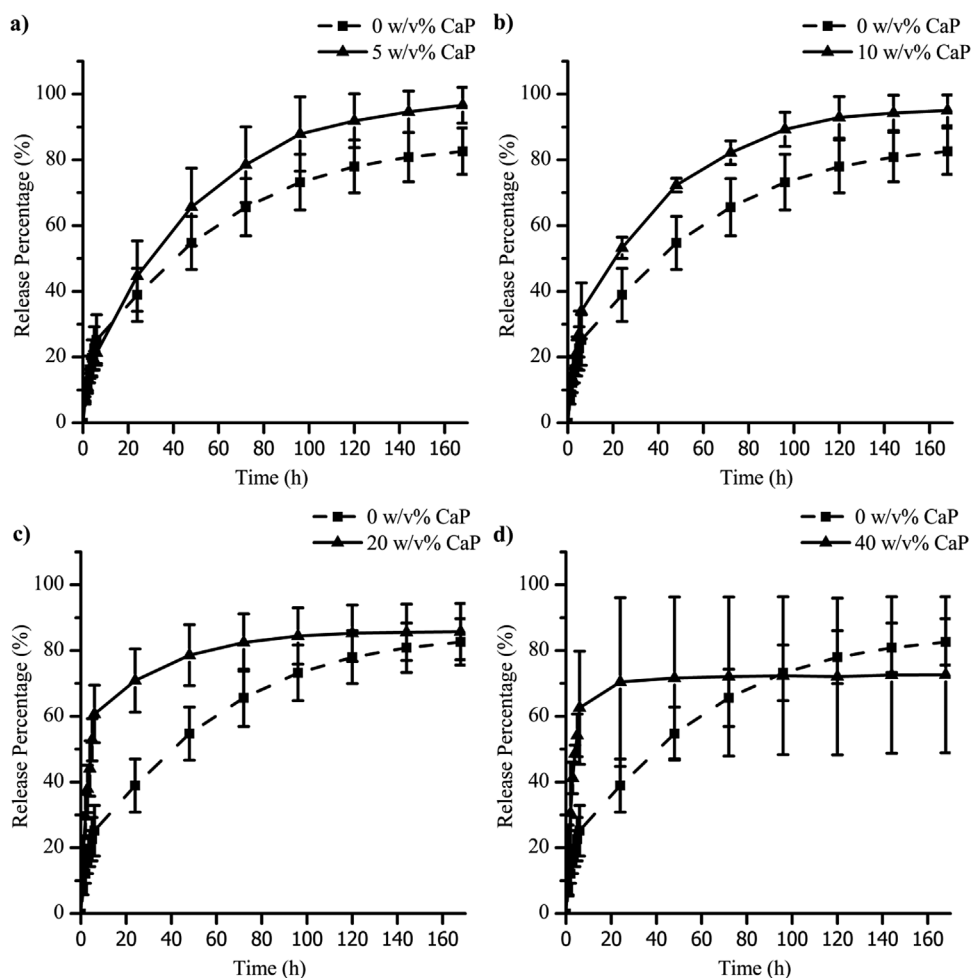


Figure 5. Drug release profiles for non-filled hydrogel as compared to hydrogel-bioceramic composite containing (a) 5, (b) 10, (c) 20, and (d) 40 w/v% CaP. ($*P < 0.05$).

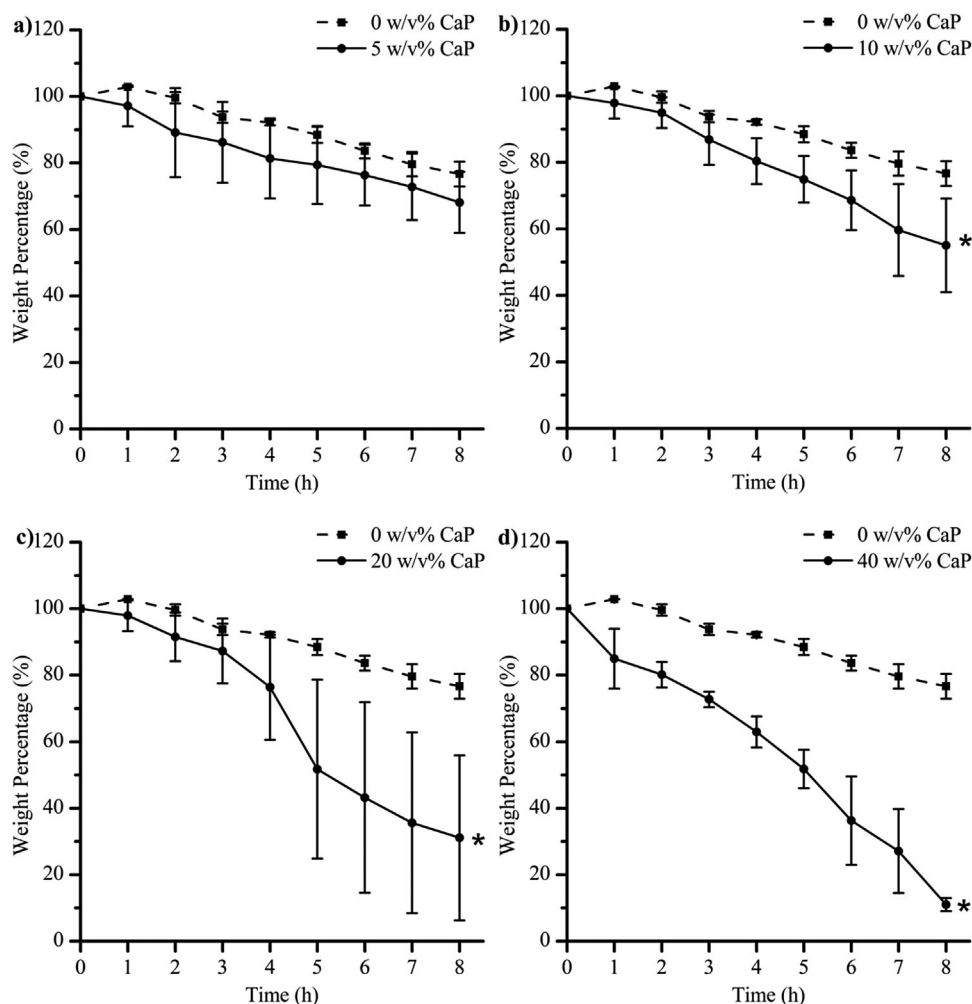


Figure 6. Degradation profile of non-filled Gtn-HPA/CMC-Tyr hydrogel compared to hydrogel-bioceramic composite containing (a) 5, (b) 10, (c) 20, and (d) 40 w/v% CaP when exposed to $0.7 \text{ U} \cdot \text{ml}^{-1}$ of type-I collagenase at 37°C . (* $P < 0.05$).

that a higher degradation rate might occur for a larger amount of CaP incorporated (refer to Figure 6) that potentially cause a burst and unstable release of the drug in particularly for the 40 w/v% CaP (with a large standard deviation for the release profile). Overall, the hydrogel-bioceramic composites incorporated with 20 and 40 w/v% CaP resulted in a sudden release of drug that could cause overdose issues. Thus, hydrogel-bioceramic composites incorporated with 5 and 10 w/v% CaP were more suitable to be used as the drug or biomolecule delivery vehicle.

3.7. Enzymatic Degradation Behavior of the Hydrogel-Bioceramic Composite

The hydrogel-bioceramic composite mainly consists of gelatin, which undergoes proteolysis *in vivo* when in contact with type-I collagenase.^[19,32] Thus, type-I collagenase was used in the current *in vitro* degradation study of the hydrogel-bioceramic composites, so that the effect of

different w/v% CaP on the degradation rate of hydrogel-bioceramic composites could be investigated. After exposure of the samples to type-I collagenase (Figure 6) for 8 h, the non-filled Gtn-HPA/CMC-Tyr hydrogel and the hydrogel-bioceramic composites with 5 w/v% CaP have a similar weight loss of 23.4 ± 3.7 and $31.9 \pm 9.2\%$ respectively. The hydrogel-bioceramic composites with 10, 20, and 40 w/v% CaP manifested a significantly ($P < 0.05$) higher degradation rate as compared to non-filled Gtn-HPA/CMC-Tyr hydrogel and underwent a weight loss of 45.0 ± 14.1 , 68.9 ± 24.9 , and $89.0 \pm 2.0\%$, respectively. This is in agreement with assumption previous made in Section 3.6, where a higher CaP amount resulted in a faster degradation behavior. Although CaP could act as the filler to improve mechanical properties, the presence of excessive CaP could also facilitate as defect sites, which is probably why the degradation rate increased with increasing w/v% CaP. In addition, excessive CaP would disrupt the covalent cross-linking of the hydrogel system, rendering it susceptible to disintegration.^[33] This

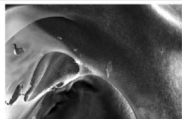
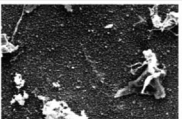
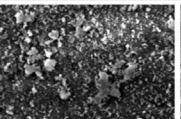
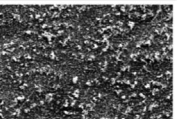
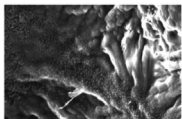
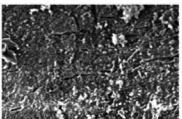
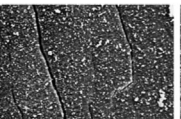
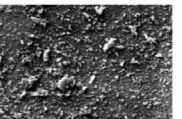
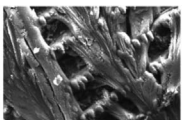
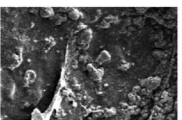
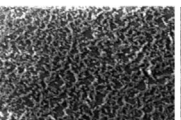
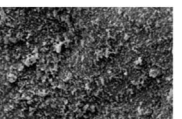
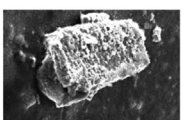

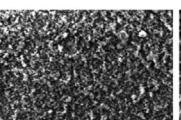
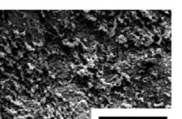
Weight Percentage of CaP (w/v%)	No Treatment	Pre-treatment	Day 1	Day 7
0	 N.A.	 0.85 ± 0.19	 1.13 ± 0.04	 1.19 ± 0.07
5	 N.A.	 0.93 ± 0.11	 1.12 ± 0.04	 1.18 ± 0.06
10	 N.A.	 0.79 ± 0.15	 1.07 ± 0.04	 1.22 ± 0.02
20	 N.A.	 0.81 ± 0.15	 1.07 ± 0.04	 1.17 ± 0.05

Figure 7. SEM images of the different groups of lyophilized samples before and after surface treatment. The Ca/P ratio of the newly formed calcium phosphate particles for each sample is indicated below every SEM images (N.A. = not applicable). (Scale bar = 50 μm).

phenomena could be observed by comparing the degradation behavior of the non-filled Gtn-HPA/CMC-Tyr hydrogel and hydrogel-bioceramic composites. Hydrogel-bioceramic composite with 5 w/v% CaP had a very similar degradation profile compared to the non-filled Gtn-HPA/CMC-Tyr hydrogel, showing that the 5 w/v% CaP was not effective in significantly disrupting the cross-linking between the hydrogel networks. As the amount of CaP increased, a higher degradation rate with an increasing standard deviation was observed, especially for the hydrogel-bioceramic composite with 20 and 40 w/v% CaP. This clearly manifests that incorporation of a high amount of CaP powder can severely compromise the structural integrity of the hydrogel-bioceramic composites. Thus, an optimal amount of CaP is crucial to improve the overall performance of the hydrogel-bioceramic composite. From the degradation results, a rapid degradation rate was observed for the hydrogel-bioceramic composite with 40 w/v% CaP, resulting in a massive loss in material and hence structural integrity. Therefore, this sample group was not suitable as an implantable scaffold and excluded from further functional studies.

3.8. Biomineralization Study

The biomineralization study was undertaken to investigate the osteocompatibility and the bioactivity of the hydrogel-

bioceramic composite by exposing the samples to 1 \times SBF. Figure 7 shows SEM images of the distribution of CaP and the Ca/P ratios of the precipitation found on both non-filled Gtn-HPA/CMC-Tyr hydrogel and hydrogel-bioceramic composites after surface treatment with 1 \times SBF. After the pretreatment process, fine minerals with a Ca/P ratio < 1.00 were deposited on all the samples. After one day of 1 \times SBF treatment, the newly formed CaP particles underwent nucleation and growth on both the non-filled Gtn-HPA/CMC-Tyr hydrogel and hydrogel-bioceramic composites reaching a Ca/P ratio of 1.13 ± 0.04 , 1.12 ± 0.04 , 1.07 ± 0.04 , and 1.07 ± 0.04 for non-filled, 5, 10, and 20 w/v% CaP, respectively. At day 7, the CaP minerals continued to nucleate and grow to an average Ca/P ratio of 1.19 ± 0.07 , 1.18 ± 0.06 , 1.22 ± 0.02 , and 1.17 ± 0.02 for non-filled, 5, 10, and 20 w/v% CaP, respectively. Overall, all samples encouraged the formation and nucleation of CaP minerals with a similar nucleation rate throughout the whole 1 \times SBF treatment, which demonstrated the suitability of the current material in bone applications due to their positive bioactive properties to integrate with the surrounding bone tissue.

3.9. 3D Cell Encapsulation Study

As seen in Figure 8a, the cells remained viable after encapsulation and started to proliferate after day 1 for all

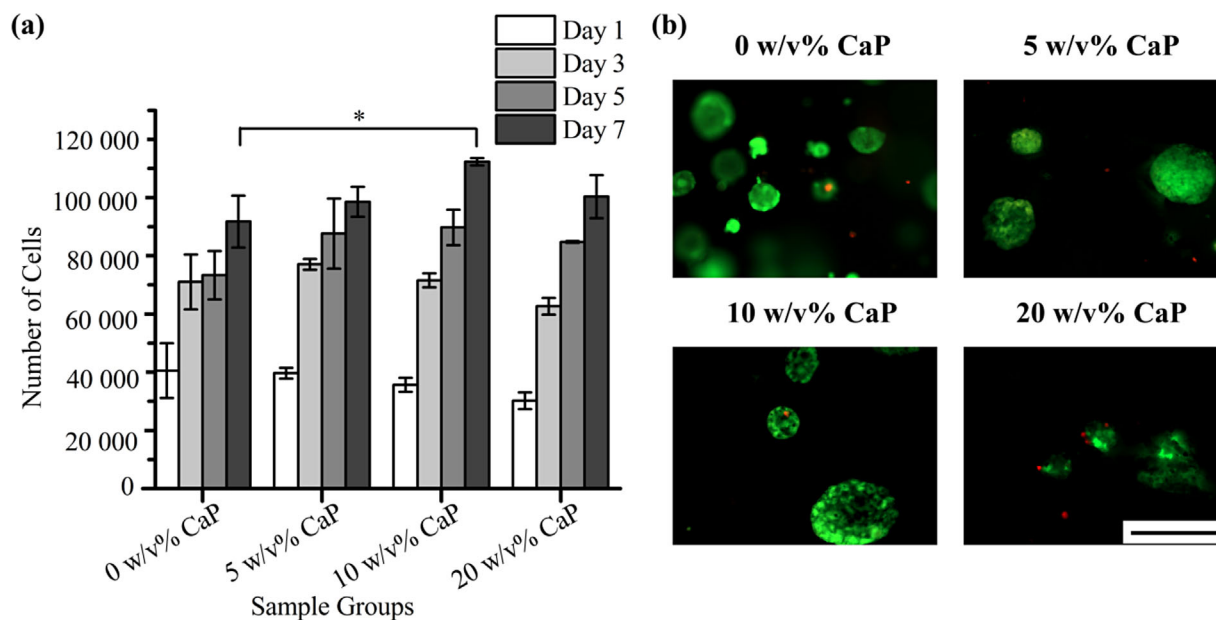


Figure 8. Effect of incorporation of calcium phosphate into the hydrogel system on (a) cell proliferation and (b) cell viability using the PrestoBlue assay ($*P < 0.05$) and LIVE/DEAD cell viability assay (green fluorescence = live cells; red fluorescence = dead cells), respectively. (Scale bar = 2 mm).

the sample groups. On day 7, the hydrogel-bioceramic composites with 5 and 20 w/v% CaP had a similar number of cells compared to the non-filled Gtn-HPA/CMC-Tyr hydrogel. However, a significant ($P < 0.05$) increase in the number of cells in the hydrogel-bioceramic composite with 10 w/v% CaP content was observed, as compared to the non-filled Gtn-HPA/CMC-Tyr hydrogel and hydrogel-bioceramic composites with 5 and 20 w/v% CaP. When cells population doubling was compared, all the hydrogel-bioceramic composites exhibited higher cells proliferation rate compared to non-filled Gtn-HPA/CMC-Tyr hydrogel as shown in Figure S1. Overall, 10 w/v% CaP exhibited the highest proliferation rate and number of cells, indicating that the 10 w/v% CaP is the optimal condition as a cell carrier. From the LIVE/DEAD viability assay, images at day 7 (Figure 8b) showed that the cells remained viable after they were encapsulated with different amounts of CaP. The higher number of viable cells (green fluorescence) over the dead cells (red fluorescence) confirmed that the fish scale-derived CaP was biocompatible and that the hydrogel-bioceramic composite was able to provide a viable environment for cells to survive and proliferate. The current results suggested that 10 w/v% CaP was the optimal CaP content for the current hydrogel system, as it provided sufficient space for cells to proliferate. The hydrogel-bioceramic composite (particularly 10 w/v% CaP) with a favorable degradation rate (Figure 6) allowed the cells to proliferate without disintegrating the scaffold. Taken together, the hydrogel-bioceramic composite containing 10 w/v% CaP could be more suitable as a potential

periosteum-mimicking system to deliver cells, support cell attachment and proliferation, and ultimately contribute to bone regeneration process.

4. Conclusion

The current work showed that the incorporation of fish scale-derived CaP powder in the Gtn-HPA/CMC-Tyr hydrogel system led to significant improvement in various functional properties favorable for bone tissue regeneration. A series of systematic investigations showed that the hydrogel-bioceramic composite with 10 w/v% CaP was optimal for an enhanced mechanical property, efficient drug delivery, and a harmonized swelling ratio with its degradation rate resulted in improved cell proliferation. In addition, its positive bioactive properties encouraged the formation and nucleation of CaP minerals. Overall, this study showed that a balance between all these properties was crucial for the optimal performance of the current hydrogel-bioceramic composite, and it could be potentially useful as a periosteum-inspired injectable system to enhance bone tissue regeneration and healing.

5. Nomenclature/Abbreviations

ABAM	antibiotic-antimycotic
Ca ²⁺	calcium ion
CMC-Tyr	carboxymethyl cellulose-tyramine
CaCl ₂	calcium chloride

CaP	calcium phosphate
DI water	deionized water
DMEM	Dulbecco's modified eagle medium
EDX	energy-dispersive X-ray spectroscopy
FBS	fetal bovine serum
FITC-dextran	fluorescein isothiocyanate-dextran
Gtn	gelatin
Gtn-HPA	gelatin-3-(4-hydroxyphenyl) propionic acid
HRP	horseradish peroxidase
Gtn-HPA/CMC-Tyr/CaP	hybrid hydrogel-bioceramic composite
HCl	hydrochloric acid
H ₂ O ₂	hydrogen peroxide
HPA	3-(4-hydroxyphenyl) propionic acid
MgCl ₂ · 6H ₂ O	magnesium chloride hexahydrate
EDC	<i>N</i> -(3-dimethylaminopropyl)- <i>N</i> '-ethylcarbodiimide hydrochloride
DMF	<i>N,N</i> -dimethylformamide
NHS	<i>N</i> -hydroxysuccinimide
PBS	phosphate buffered saline
PO ₄ ³⁻	phosphate ion
KCl	potassium chloride
K ₂ HPO ₄ · 3H ₂ O	potassium hydrogen phosphate trihydrate
SEM	scanning electron microscopy
SBF	simulated body fluid
CMC	sodium carboxymethyl cellulose
NaHCO ₃	sodium bicarbonate
NaCl	sodium chloride
NaH ₂ PO ₄ · H ₂ O	sodium phosphate monobasic
3D	three dimensional
β-TCP	β-tricalcium phosphate
Tyr	tyramine
w/v%	weight per volume percent
wt%	weight percent
XRD	X-ray diffractometry

Acknowledgements: The authors would like to acknowledge the funding support from the Singapore Ministry of Education Academic Research Fund (AcRF) Tier 2 ARC16/11. This research grant is also supported by the Singapore National Research Foundation under its Environmental & Water Technologies Strategic Research Programme and administered by the Environment & Water Industry Programme Office (EWI) of the Public Utility Board (PUB).

Received: July 8, 2015; Revised: September 15, 2015; Published online: DOI: 10.1002/mabi.201500258

Keywords: biocompatibility; biomaterial; biomineralization; biopolymers; hydrogels

- [1] P. V. Giannoudis, H. Dinopoulos, E. Tsiridis, *Injury* **2005**, *36*, S20.
- [2] M. K. Sen, T. Miclau, *Injury* **2007**, *38*, S75.
- [3] R. C. Sasso, J. C. LeHuec, C. Shaffrey, *J. Spinal. Disord. Tech.* **2005**, *18*, S77.
- [4] W. R. Moore, S. E. Graves, G. I. Bain, *ANZ J. Surg.* **2001**, *71*, 354.
- [5] X. Zhang, H. Awad, R. O'Keefe, R. Guldborg, E. Schwarz, *Clin. Orthop. Relat. Res.* **2008**, *466*, 1777.
- [6] Y. Kang, L. Ren, Y. Yang, *ACS Appl. Mater. Interfaces* **2014**, *6*, 9622.
- [7] M. D. Hoffman, C. Xie, X. Zhang, D. S. W. Benoit, *Biomaterials* **2013**, *34*, 8887.
- [8] I. Manjubala, M. Sivakumar, R. V. Sureshkumar, T. P. Sastry, *J. Biomed. Mater. Res.* **2002**, *63*, 200.
- [9] L. X. Lü, X. F. Zhang, Y. Y. Wang, L. Ortiz, X. Mao, Z. L. Jiang, Z. D. Xiao, N. P. Huang, *ACS Appl. Mater. Interfaces* **2012**, *5*, 319.
- [10] A. Al-Abboodi, J. Fu, P. M. Doran, P. P. Y. Chan, *Adv. Healthc. Mater.* **2014**, *3*, 725.
- [11] N. A. M. Barakat, M. S. Khil, A. M. Omran, F. A. Sheikh, H. Y. Kim, *J. Mater. Process Technol.* **2009**, *209*, 3408.
- [12] M. Boutinguiza, J. Pou, R. Comesaña, F. Lusquiños, A. de Carlos, B. León, *Mater. Sci. Eng. C* **2012**, *32*, 478.
- [13] N. Panda, K. Pramanik, L. Sukla, *Bioprocess. Biosyst. Eng.* **2014**, *37*, 433.
- [14] A. Al-Abboodi, J. Fu, P. M. Doran, P. P. Y. Chan, *Biotechnol. Bioeng.* **2013**, *110*, 318.
- [15] T. Kokubo, H. Kushitani, S. Sakka, T. Yamamuro, *J. Biomed. Mater. Res.* **1990**, *24*, 721.
- [16] G. Daculsi, B. H. Fellah, T. Miramond, "The Essential Role of Calcium Phosphate Bioceramics in Bone Regeneration," in *Advances in Calcium Phosphate Biomaterials*, B. Ben-Nissan, Ed., Springer, Berlin, Heidelberg, Germany **2014**, p. 71.
- [17] P. X. Ma, J. Elisseeff, "Scaffolding In Tissue Engineering," CPC Press, Boca Raton, FL, USA **2005**.
- [18] L.-S. Wang, C. Du, J. E. Chung, M. Kurisawa, *Acta Biomater.* **2012**, *8*, 1826.
- [19] L. S. Wang, J. E. Chung, P. P. Y. Chan, M. Kurisawa, *Biomaterials* **2010**, *31*, 1148.
- [20] K. M. Park, K. S. Ko, Y. K. Joung, H. Shin, K. D. Park, *J. Mater. Chem.* **2011**, *21*, 13180.
- [21] J. A. Burdick, G. D. Prestwich, *Adv. Mater.* **2011**, *23*, H41.
- [22] D. L. Elbert, *Acta Biomater.* **2011**, *7*, 31.
- [23] Q. L. Loh, C. Choong, *Tissue Eng. Part B. Rev.* **2013**, *19*, 485.
- [24] R. A. Gittens, T. McLachlan, R. Olivares-Navarrete, Y. Cai, S. Berner, R. Tannenbaum, Z. Schwartz, K. H. Sandhage, B. D. Boyan, *Biomaterials* **2011**, *32*, 3395.
- [25] F. M. Watt, W. T. S. Huck, *Nat. Rev. Mol. Cell Biol.* **2013**, *14*, 467.
- [26] Y. K. Wang, C. S. Chen, *J. Cell Mol. Med.* **2013**, *17*, 823.
- [27] H. Sun, F. Zhu, Q. Hu, P. H. Krebsbach, *Biomaterials* **2014**, *35*, 1176.
- [28] A. S. Reddy, G. N. Sastry, *J. Phys. Chem.* **2005**, *109*, 8893.
- [29] A. T. Neffe, A. Loebus, A. Zaupa, C. Stoetzel, F. A. Müller, A. Lendlein, *Acta Biomater.* **2011**, *7*, 1693.
- [30] D. Bhatnagar, D. Gersappe, J. C. Sokolov, M. H. Rafailovich, J. Lombardi, *Macromolecules* **2015**, *48*, 840.
- [31] Y. S. Pek, M. Kurisawa, S. Gao, J. E. Chung, J. Y. Ying, *Biomaterials* **2009**, *30*, 822.
- [32] K. A. Murphy, "Regulation of Matrix Metalloproteinase Expression and Activity by the Aryl Hydrocarbon Receptor in A2058 Human Melanoma Cells," Rutgers The State University of New Jersey, ProQuest **2008**.
- [33] J. P. Lewicki, M. Patel, P. Morrell, J. Liggit, J. Murphy, R. Pethrick, *Sci. Technol. Adv. Mater.* **2008**, *9*, 1.